Tellus (1984), *36A*, 369–383

Observations of a mountain-wave event over the Pyrenees

By KLAUS P. HOINKA, *Institute of Atmospheric Physics, German Aerospace Establishment (DFVLR), D-8031 Oberpfaffenhofen, Federal Republic of Germany*

(Manuscript received December 28, 1982; in final form August 19, 1983)

ABSTRACT

An analysis of data obtained from instrumented aircraft is performed. These data were gathered on flights in a mountain wave above the Pyrenees during ALPEX on March 23, 1982. The observed two- and three-dimensional thermal and dynamical structure of the flow is presented. Beneath 7 km altitude, strong three-dimensional response in the atmosphere can be seen in the wind and temperature fields. It appears that the response is almost two-dimensional above this height. Rather pronounced lee waves are found in the lower troposphere. Moreover, a mountain wave with moderate amplitude is apparent, which becomes stronger with reversed phase near the tropopause. The phaselines of the waves are tilted vertically upstreamwards indicating downward flux of momentum. Another observed feature is the destabilization of the troposphere in the lee of the barrier. Emphasis is placed on the determination of the downward flux of momentum due to the waves.

1. Introduction

There are numerous observations of atmospheric features above mountains of the scale of the Rocky Mountains (Kuettner and Lilly, 1968; Lilly and Kennedy, 1973; Lilly, 1978). Smaller scale mountains such as the Alps, the Pyrenees and the Yugoslavian coastal mountains also have strong dynamical and thermal influence on atmospheric flows. Flows over these mountains, however, are observed and documented to a much lesser extent than those for large-scale mountains. One of the objectives of the 1982 GARP experiment ALPEX was to obtain observational data of the atmosphere above the Alps, in particular to measure the transport of momentum between the atmosphere and the earth over a limited terrain region. Preliminary ALPEX results on airflow pattern over the Yugoslavian coastal mountains, over the Alps and over the Pyrenees were reported by Kuettner (1982).

During ALPEX, a data-gathering flight was made over the Pyrenees on March 23, 1982. The Pyrenees are located at the border between France and Spain touching the Mediterranean Sea as well as the Atlantic ocean. The approximate mean height is 2000 m, maximum height is 3200 m. This paper is a report on the mountain-wave event over the Pyrenees on March 23, 1982. A first cross section of the thermal structure was presented by Hafner (see Kuettner, 1982). To make an analysis, he assumed steady state and two-dimensional behaviour of the airflow over the Pyrenees on March 23, 1982. However, the various flight tracks used were approximately 80 km apart and additionally a long separation in time up to 4 h between the various legs may lead to some uncertainty and ambiguity in the analysis of Hafner. Therefore, in the present paper, we determine how far the assumptions of two-dimensionality and steadiness are valid for the present event. The first objective is to describe as completely and accurately as possible the dynamical and thermal three-dimensional structure of the airflow over the Pyrenees.

One of the most important quantitative measures of mountain wave intensity is the exchange of momentum between the atmosphere and the orography. Lilly and Kennedy (1973) and Lilly (1978) determined for a moderate- and a strong-wave event above the Colorado Rockies the magnitude of energy exchange between the atmosphere and the Rockies. For small-scale topography, i.e. the Appalachians, Smith (1978) has

reported the magnitude of the momentum exchange. But for a barrier of the scale of the Pyrenees, similar information does not exist. A second objective of this paper is to determine the exchange of momentum between the atmosphere and a barrier of this scale.

2. The synoptic structure

In Fig. 1 (bottom) the synoptic situation at 300 mb of March 23, 1982 is plotted. In the upper troposphere, a ridge of high pressure is located west of Spain. Above the Alps a trough of low pressure is observed. This synoptic structure leads to northerly flow in the mid- and upper-troposphere above the Pyrenees. The top figure shows the surface pressure chart with a ridge of high pressure above Great Britain and a surface trough located above the easter Mediterranean Sea. Therefore, in the region of interest we may expect cross isobaric flows close to the surface. In Fig. 2, a satellite picture shows the area of interest with Spain at the left edge. Above and north of the Pyrenees there are low-level clouds. South of the Pyrenees there are no clouds, with a sharp boundary in the lee. This indicates that at the leeward side, a subsidence in the atmosphere has occurred leading to a decrease in cloudiness. In summary, the synoptic structure shows a flow perpendicular to the barrier of the Pyrenees and therefore, mountain wave and foehn features are expected to be observed.

To give a rough estimate of the basic-state properties upstream north of the Pyrenees, a composite sounding is given in Fig. 3. The rawinsonde data of Trappes, Bourges, Lyon, Bordeaux and Toulouse (all France) were used to establish the basic characteristics of the upstream flow.

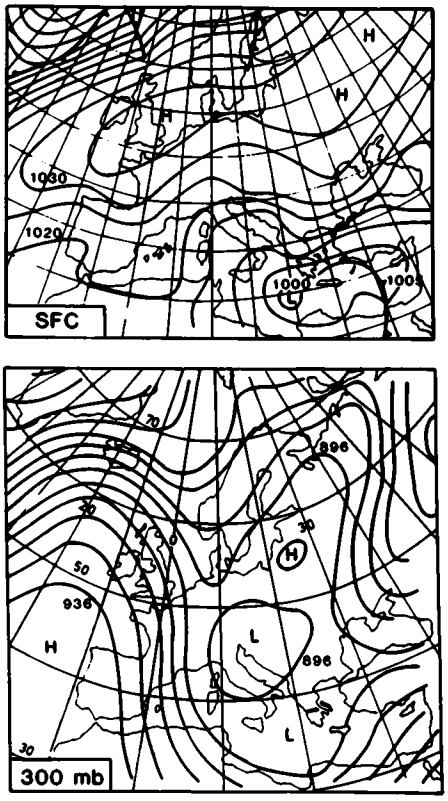

Fig. 1. Surface pressure chart (top) and 300 mb chart (bottom) for March 23, 1982. The increment of pressure in the surface chart is 5 mb. The increment at 300 mb is 8 gpm.

3. The data

On March 23, 1982, two instrumented aircraft made data-gathering flights over the Pyrenees between Toulouse (France) and Barcelona (Spain), one four-engine aircraft, the NOAA P-3 and the DFVLR jet FALCON. The flight levels for which useful data are available are shown as the horizontal dashed lines on Figs. 6–10. A brief sketch of the flight pattern is presented in Fig. 4. It is a west-east cross section. The FALCON covered the layer between 9 km and 13 km touching and crossing several times the tropopause. The P-3 covered the mid to lower tropospheric region. The crosses indicate northward flight tracks, the dots stand for southward flight tracks. Additionally, the starting and ending times (in GMT) of the cross flights are given. The locations of the different cross flights were approximately 80 km apart.

Fig. 4 highlights the rather large spatial and time differences between the various flight tracks. So, one has to be very careful in analysing the present data whenever, the observed phenomena are non-stationary and not two-dimensional. The response of the atmosphere on orographic forcing

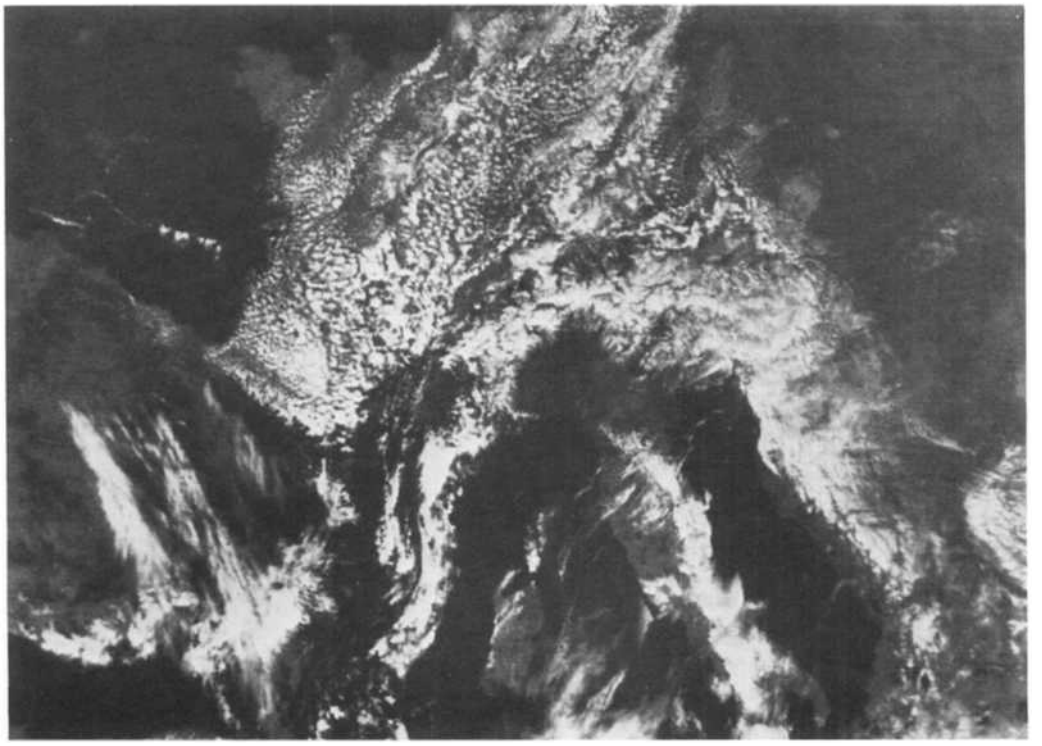

Fig. 2. Satellite picture (NOAA 7, AVHRR channel 2) at March 23, 1982 1320 GMT. Spain is located at the left-hand edge.

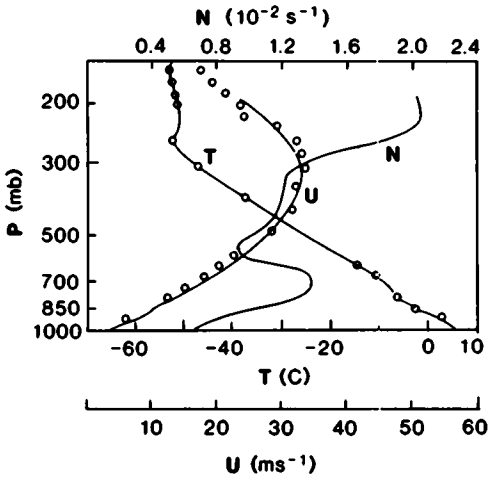

Fig. 3. Composite sounding north of the Pyrenees on March 23, 1982 1200 GMT for wind speed u (normal to the Pyrenees), temperature T and Brunt-Väisälä frequency N as a function of pressure p. This sounding was constructed by Karl Cox in conjunction with the study by Blumen and Cox (1983).

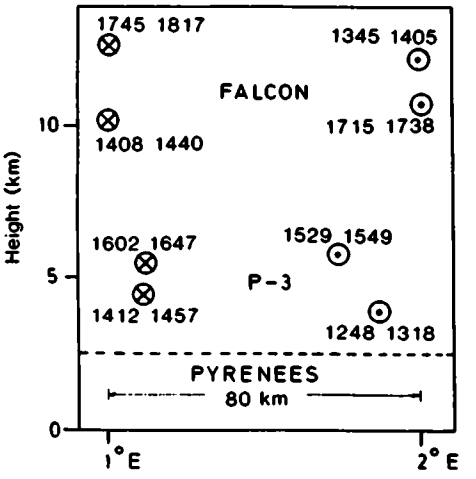

Fig. 4. West-east cross section above the Pyrenees showing schematically the flight patterns of the DFVLR-aircraft FALCON and the NOAA-aircraft P-3. The crosses indicate northerly flight tracks while dots stand for southerly tracks. Note the times in GMT of the start and end of the cross flights. The abscissa is given in degrees of longitude.

depends strongly on the type of orography. The north-south profiles of the Pyrenees at 1° E and 2° E are given in Fig. 5. The profiles show the maximum height along the sections. Maximum height in the near vicinity (approx. 10′ east and west of the profiles) are indicated by stars (1°) and triangles (2°). At the southern side of both profiles, various additional smaller barriers can be seen. One can say that the 2° profile has a smoother behaviour than the 1° profile, which has the additional ridge of the Sierra del Montsech close to 42°. The main ridge (between 43° and 42°30′) of the 1° profile is broader than the 2° profile. All these differences should result in different flow patterns in the lower troposphere. However, detailed information on the atmospheric response to complex terrain is not available.

Instrumentation and output data available from both aircraft are described briefly by Kennedy (1982). The accuracy of the instrumentation and recorded data is also mentioned to some extent by Kennedy. The absolute accuracy of temperature is 0.2 K, of pressure 0.15 mb (P-3) and 0.25 (FALCON), of the horizontal wind components 1.0 ms $^{-1}$ (P-3) and 1.5 ms $^{-1}$ (FALCON) and of the vertical wind component 0.5 ms^{-1} (both aircraft). For the FALCON, the relative errors of temperature are 0.05 K, of wind speed 0.1 ms^{-1} and of static pressure 0.25 mb. The data of the FALCON are originally 10 Hz data; after filtering out very high frequencies, greater than 1 Hz, averaged values for every second are produced. Depending on the true ground speed, an averaged value over a second is representative for a horizontal distance between 100 m and 250 m. A further averaging over 10 s was useful for most of the calculations

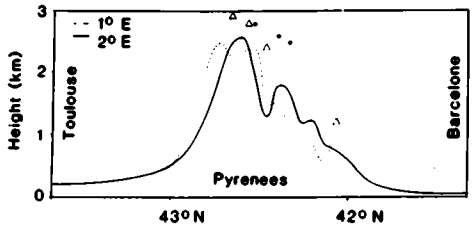

Fig. 5. The north to south mountain profiles of the mean height crossing the Pyrenees at 1° E (dashed) and 2° E (full) with maximum heights in the near east-west vicinity of 10′ of the profiles. The stars (triangles) stand for those close to the 1° (2°) E. The height at the ordinate is given in km, the abscissa is given in degrees longitude.

presented. The data available from the P-3 are mean values over a time of 1 s.

Vertical soundings are available from rawinsonde observations at Toulouse (France) (00 and 1200 GMT). Additionally, the P-3 has made a descent near Toulouse (France) and the FALCON a descent and ascent between Bordeaux (France) and Toulouse (France). Toulouse is located north of the Pyrenees (43°40′ N) and Barcelona is located south of the barrier (41°20′ N).

4. The mesoscale structure

Since the cross sections differ with respect to orographic profiles, one must expect different atmospheric responses above the Pyrenees. Therefore, it is preferable in this section to discuss the two different cross sections at 1° E and 2° E separately, and a combination of both. The purpose is to see how far the assumption of two dimensionality is valid for the present event. For reasons of simplicity we assume steadiness, although there is a long separation of time (>3 h) between the various legs, which may lead to some uncertainty.

The observed isentropic fields are given in Fig. 6. The top (bottom) figure shows the structure at 1° E (2° E). The cross sections are oriented north-south with north to the left. Thus, the flow comes from the left. The distance between 41° N to 44° N is approximately 330 km. Note, that the increment for the isentropes is 1 K below 305 K and 5 K above 305 K. The isentropic patterns in the data gap region between 6 km and 9 km are estimated by subjective analysis according to the data above and beneath this region.

In both cases, a northerly flow without waves approaches the barrier and the analysis shows the flow southward from 41°30′ also to be without waves. Although there is a gap in the data of the troposphere, several significant features can be seen. In both cases, we see that at the lee side in the layer between 6 and 12 km, the differences in height of the isentropes are greater than at the windward side. For example, the difference in height between the 330 K and the 303 K isentrope at the windward side is 4 km and at the leeside 5 km (2° E). For the 1° cross section, height differences of 5.5 km (lee) and 4 km (windward side) are analysed. This means that the mid-tropospheric

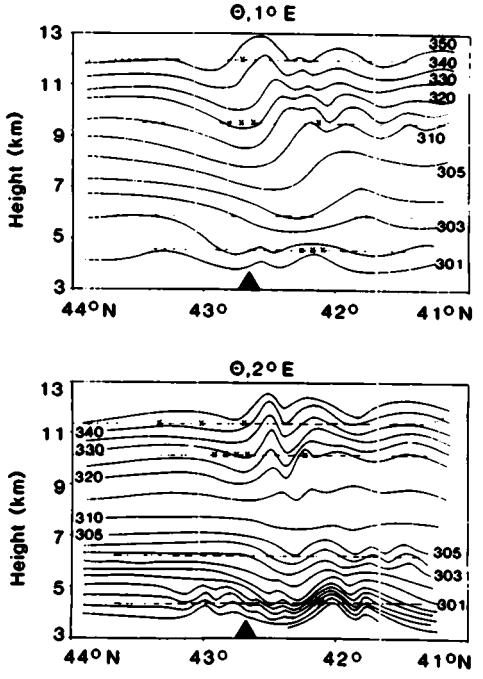

Fig. 6. Cross sections of potential temperatures in K along a north-south line between 44° N and 41° N for March 23, 1982. The top (bottom) figure shows the structure along 1° (2°)E. Note, that the increment above 305 K is 5 K while beneath 305 K it is 1 K. The dashed lines indicate the flight legs. The abscissa is given in degrees latitude, the height at the ordinate is given in km. The scale between 41°N and 44°N is approximately 330km. The black triangle indicates the approximate location of the main ridge. The crosses mark regions, where light to moderate turbulence was encountered.

atmosphere in the lee of the mountain is less stable than that at the windward side. Similar leeward-side opening of the streamlines is observed above the Rockies occurring during strong chinook (Lilly, 1978) and during foehn in the Alps.

In the lower troposphere, remarkable differences in the 1° and 2° cross section in the isentropic fields can be seen. There is only one wave visible at 1° and a train of small-scale waves at the 2° cross section with a wavelength of 15 km upstream and above the barrier between 43° and 42°30′. These waves are popularly known as lee waves. In the upper troposphere and in the lower stratosphere, a double-wave close to 42°30′ with an amplitude of 1.5 to 2 km is observed in both cases. Note the vertical tilt upstreamwards of the phaselines indicating a downward flux of horizontal momentum. In the upper troposphere, a wave with moderate amplitude above the ridge can be seen in both cross sections followed by a second wave. This wave has different phases for both cross sections.

The crosses in Fig. 6 mark regions with light to moderate turbulence. Most of the observed turbulence was of light character. Close to the tropopause, turbulence was encountered above the barrier or in the near upstream area. In the lower troposphere, moderate turbulence was encountered just in the lee region.

The northerly wind component is given in Fig. 7. For reasons of simplicity, the northerly wind component v is henceforth taken as positive for winds coming from north. We see in the mid-troposphere a broad region with 35 ms^{-1}. Close to the mountain an increase up to 45 ms^{-1} (2° E) can be seen followed with a small region of lower velocities (<35 ms^{-1}) and a further increase to 40 ms^{-1}. In the 1° E case, a flow with 40 ms^{-1} approaches the barrier between 6 and 12 km altitude. In the lee, no significant increase is

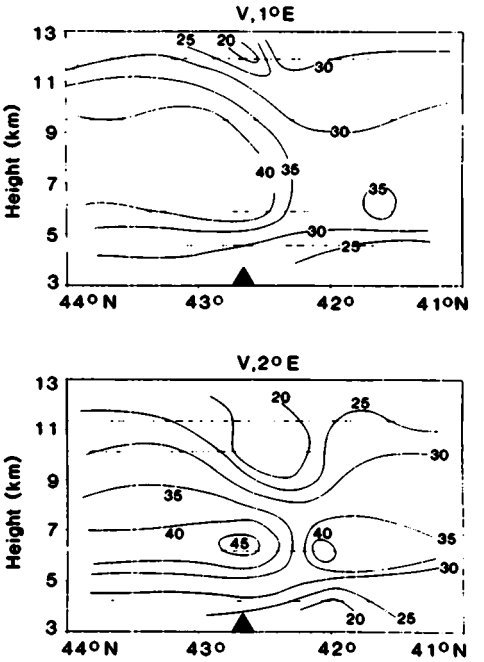

Fig. 7. As in Fig. 6, except for the northerly wind component in ms^{-1}. Note, that v greater than zero represents winds from north.

analysed. In both cases in the upper troposphere, a decrease is observed down to 20 ms^{-1} related to the strong wave formation close to the tropopause.

The observed pattern shown in Figs. 6b and 7b is fairly close to the circulation above the Colorado Rocky Mountains observed and reported by Lilly and Kennedy (1973), (Fig. 1 in their paper). Henceforth we refer to this event as the "Colorado-case". They found above the Rockies on February 17, 1970 small-scale lee waves (wavelength approximately 15 km) at 7 km altitude and a significant wave with an amplitude of 2 km above the mountain at 15 km height. The height differences between our case and the Colorado-case are due to the fact that the plains east of the Rockies and the area west of the Continental Divide are one mile high, so presumably the response of the atmosphere is found to be one mile higher than above the Pyrenees. The agreement between the Colorado-case and the wave event above the Pyrenees is the result of a qualitative comparison of both circulation patterns. A closer examination shows that the mean atmospheric Brunt-Väisälä frequency for the Colorado-case is 0.015 s^{-1}, which is fairly close to that of 0.012 s^{-1} of the Pyrenees-case (see Fig. 3). The wind profiles were similar with wind increasing up to 10 km above ground and decreasing above. The magnitude of the maximum winds is quite different: 35 ms^{-1} (Pyrenees) and 60 ms^{-1} (Colorado-case). This leads to differences in the characteristic vertical wavelengths: 14 km (Pyrenees) and 18 km (Colorado). These estimates, however, are somewhat ambiguous for realistic flows, because the evaluation of the mean stability and the mean wind is not that clear. Another observed case similar to the presented flow is reported by Kuettner and Lilly (1968). However, the features are not as striking as those in the Colorado-case.

Finally, in Fig. 8, the zonal wind component field is plotted. A remarkable feature is that at the windward side there is an eastwind component, since at the leeward side a westwind component is observed.

When analysing two-dimensional cross sections, one should pay attention to the natural variation that would be expected transverse to the jet across the barrier. The thermal wind equation requires transverse potential temperature gradients and the geostrophic equation requires transverse Montgomery potential gradients. Either a mean flow

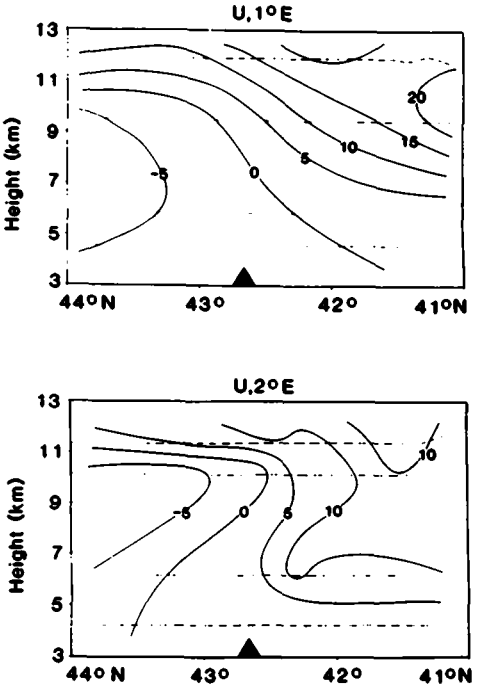

Fig. 8. As in Fig. 6, except for the westerly wind component in ms^{-1}.

misalignment or perturbation transverse advection could bring variations into the section which could not be explained in two dimensions. This problem has been the cause of incorrect analysis in the past. In the present case, the jet crosses almost normal to the barrier which is evident from the gradient of the isohypses at 300 mb (Fig. 1) as well as from the magnitude of meridional velocities (Fig. 8). Thus, the angle of attack of the jet is approximately 90° and the flow lies nearly in the analysed planes. A rough estimate of the transverse potential temperature gradients shows at the height of 11 km a difference of 5 K north as well as south of the Pyrenees, at 9 km 8 K (north) and 9.5 K (south), at 7 km 1.5 K (north) and 2.5 K (south) and finally at 5 km −2.5 K (north) and −0.5 K (south). All values are estimated by evaluating $\theta(2°) - \theta(1°)$. These estimates and the corresponding vertical gradients confirm that the angle of attack was close to 90°.

To get more information on the wave characteristics of the flow above the 1° and 2° mountain profiles, the corresponding time series of the data (θ)

along the flight legs were Fourier analysed. At the lower level, at 4.0 km, a significant peak was found in wave amplitude at 30 km and 15 km wavelengths. These peaks do not appear for the time series at the heights 4.5 km, 5.5 km and 5.8 km. The small difference in height (500 m) between the two lowest flight legs, the large spatial difference (80 km apart) of both legs and the apparent differences in wave characteristics suggest the strong three-dimensional behaviour of the flow at this height. However, one should keep in mind that the time separation between both legs is between 1 and 2 h. In the upper levels, no significant differences of wave properties were found. Every frequency analysis shows a strong wave disturbance of wave-length of approximate 100 km. In summary, we see strong differences in the lower troposphere for the two cross sections 80 km apart which do not allow the use of the assumption of two-dimensionality. These differences become less pronounced with increasing height.

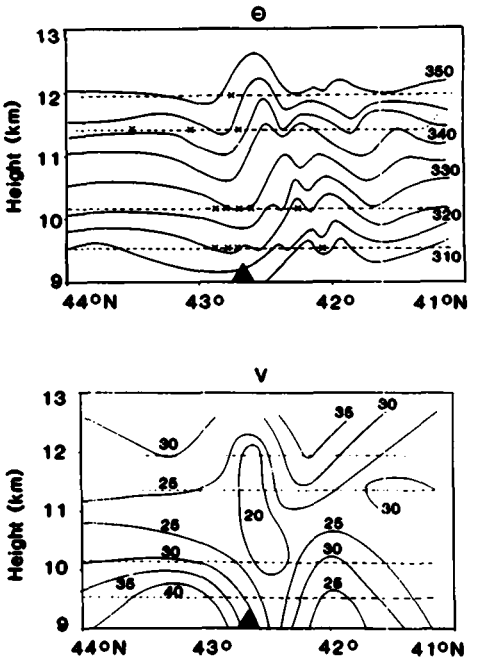

Fig. 9. Cross section of potential temperatures in K along a north-south line between 44° N and 41° N for March 23, 1982 using a combination of all FALCON legs. Dashed lines indicate the flight legs. The bottom figure shows the corresponding meridional wind field. Note that v greater than zero represents winds from the north and that just the upper part of the atmosphere from 9 to 13 km is shown. The crosses mark regions, where light to moderate turbulence was encountered.

To show the high-altitude structure, a combined analysis of the four FALCON tracks is carried out in Fig. 9. The tropopause was very close to the 315 K is isentrope. We see descent in front of the barrier followed by a significant ascent in the lee of the mountain. Rawinsonde observations during foehn above the Alps suggest that the height of the tropopause above the windward side station Milano (Italy) is lower than above the lee station Munich (Hoinka, 1980). The author has reported a mean pressure difference at the tropopause between Munich (224 mb) and Milano (229 mb) of 5 mb during south foehn. In the horizontal windspeed, a decrease is apparent in the region of the strong wave (Fig. 9, bottom).

Finally, in Fig. 10 a zoomed part of the FALCON observations between 42° and 43° is given. The dashed lines stand for the isentropes and the full lines give the vertical velocities. This w-θ pattern corroborates qualitatively that in the case of the derivatives $d\theta/dx < 0$ we find $w > 0$ and vice versa. This means to some extent that the streamlines and the isentropes coincide, with the consequence that the assumption of steadiness and two-dimensionality is allowed for the upper levels in the present case.

5. Potential temperature and velocity results

In this section we will discuss potential temperature and wind pattern along two selected flight tracks. One track represents the lower troposphere to show the behaviour of the variables in the lee wave region. This is the lowest track operated by the P-3 at 4.0 km altitude. A similar flight track has been discussed by Lilly and Kennedy (1973). In their case, it was the level of 6.4 km which is one mile higher than our chosen level but corresponds well to ours as discussed in the previous section. So, we can compare our results with those of the Colorado-case. Additionally, we will present the behaviour of the variables close to the tropopause at 11.4 km altitude.

In Fig. 11, the potential temperature (thin lines), northerly wind component (11a) and vertical air velocity (11b) are drawn for the low-level track.

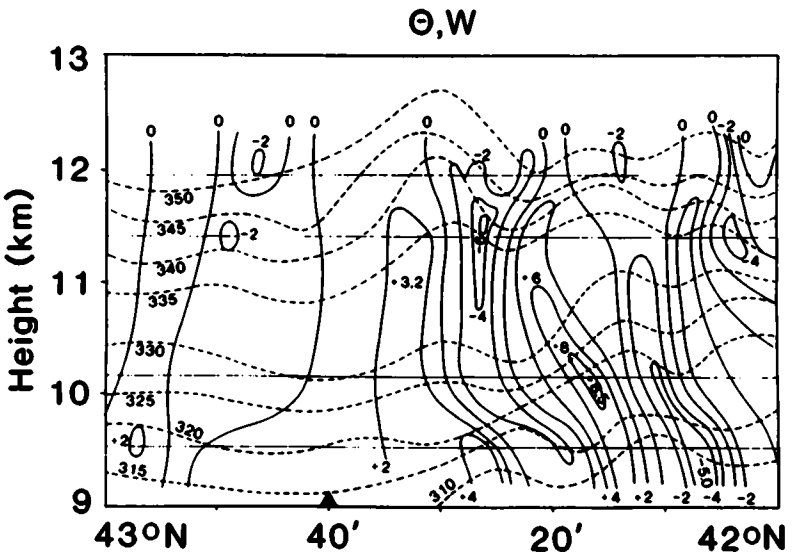

Fig. 10. Cross section of vertical velocity (full lines) in ms ' and potential temperature (dashed lines) in K for all FALCON legs between 42° N and 43° N of the March 23, 1982. The flight legs are indicated by thin lines.

Close to the mountain, the potential temperature oscillates with amplitudes of 6–9 K. In the Colorado-case, there was only one significant decrease of 10 K close to the mountain. The oscillating pattern is reflected in the behaviour of the vertical airspeed with small amplitude waves above the barrier and strong variation in vertical velocity in the lee. The magnitude of the horizontal wind component increases from an averaged value of 28 ms ' to 20 ms^{-1} at the lee side with an increase to 25 ms ' in the further lee. A similar behaviour was observed in the Colorado-case.

In Fig. 12, the potential temperature (thin lines), northerly wind component (12a) and vertical air velocity (12b) are plotted for the 11.4 km level. Again, a remarkable decrease in θ of 10–15 K is observed above the barrier. In the Colorado-case, an amount of approximately 18 K was observed. The magnitude indicates that these tracks are located in the lower stratosphere. In the horizontal windfield, a decrease from 30 to 20 ms^{-1} can be seen close to the mountain. In the further lee, an oscillating behaviour was again analysed. Note, that u and θ are almost in phase in the lower troposphere, since the contrary is true in the lower stratosphere. The magnitude of the w-amplitude is half the amount observed in the lower troposphere. This result is consistent with (slightly leaky) lee wave theory. Below the height of maximum lee wave amplitude, v and θ are in phase as the streamlines are closer together in the trough. In the present case, the maximum lee wave amplitude may occur above the level of 4.0 km. Above the level where the maximum lee wave amplitude occurrs, the reverse is true, as the streamlines are further apart in the trough. The wave is slightly leaky as the momentum flux remains negative. If this interpretation is correct, then there was a nearly trapped wave between the upper (11.4 km) and the lower 4.0 km) flight levels. We see from Figs. 11–12 that the character of the fields of potential temperature, northerly and vertical velocity is generally one of one long wave with superimposed small-amplitude (windward) and large-amplitude (lee) ripples.

Some additional information on the character of the flow is obtainable from considerations of the power and correlation spectra. In order to get these results, we removed from the data the mean and trend by least-squares fitting. From these transformed variables, we calculated the power spectra of θ, v and w and the correlation spectra for each pair of variables (v-θ, w-θ, v-w). The results are presented in Figs. 13–17 for the two flight tracks in 4.0 and 11.4 km.

The power spectra in Fig. 13 (for 4.0 km) and

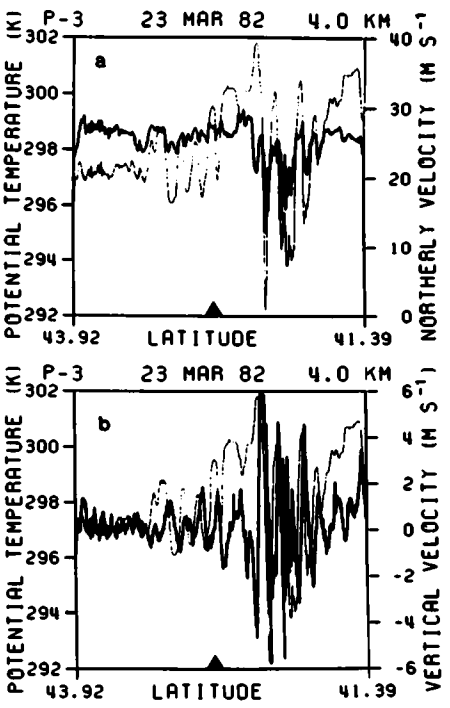

Fig. 11. Potential temperature (thin), northerly winds ((a), solid) and vertical velocity ((b), solid) from the P-3 flight record at the 4.0 km level. The mountain crest is indicated by the black triangle.

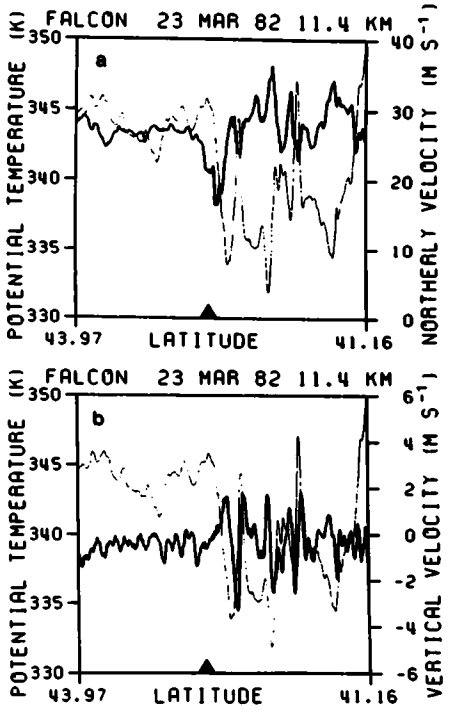

Fig. 12. As in Fig. 11 except for the FALCON flight record at 11.4 km level.

Fig. 14 (11.4 km) suggest the existence of a k^{-3} slope for the larger scales. A $k^{-5/3}$ slope in the smallest wavenumber decade is present for the lower flight track. In the lower stratosphere case, a shallower slope, perhaps a $k^{-5/3}$ slope, is evaluated only for θ. This is because the θ-values are the originally measured values which consist of turbulence characteristics up to frequencies of 10 Hz. The wind data are derived from the measurements of an inertial platform and of a direction-sensitive Pitot-tube. The final data are derived by applying a filter which smooths out frequencies greater than 1 Hz. So, the $-5/3$ slope cannot be seen in the power spectrum of the wind data. In both levels for all variables, we see a slight decrease of the slopes at the lower end of the frequencies, which indicates that existing trends are not removed completely.

In Figs. 15–17, we show the phase of the correlation spectra v versus θ, w versus θ and v versus w. A positive phase $<180°$ signifies that the first-named variable leads the second in time. In the present study, the degree of freedom in the spectrum analysis is approximately 20. Thus following Julian (1975) we get a limiting coherence of 0.28 for a probability level of 95%. For this level, all phases are exact with a deviation of $\pm 60°$.

A simple solution for a large-scale gravity wave would yield a v pattern being out of phase with θ, corresponding to a phase near 90°, where θ lags v. This behaviour is apparent at the 11.4 km level (Fig. 15), whereas at 4.0 km, v and θ are almost in phase. These phase relationship results confirm the structure shown in Figs. 11 and 12. The coherences (not shown) are high with 0.4 (4.0 km) and 0.2 (11.4 km) for low frequencies.

For a stationary gravity wave, we expect that θ leads w with a phase of $+90°$. The phase patterns for both levels apparently indicate this behaviour (Fig. 16). We find a phase of $-90°$ for the correlation w versus θ which is a phase of $+90°$ for v versus w. Another significant corroboration is to be seen in Fig. 10, where the pattern of θ and w

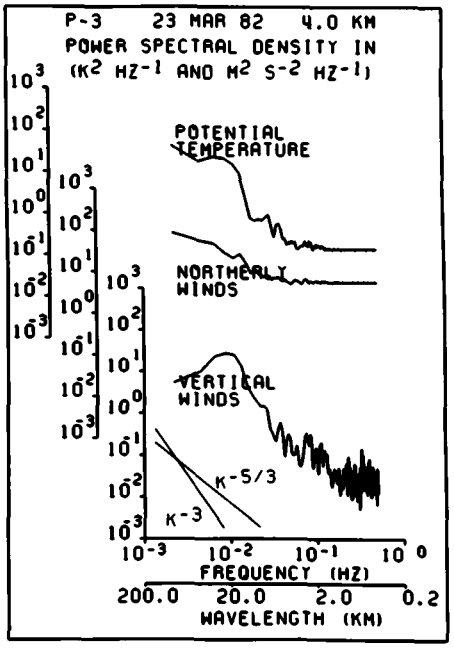

Fig. 13. Power spectra of potential temperature, vertical velocity and northerly velocity for the 4.0 km flight level of the P-3. The abscissa and ordinate are labelled in terms of frequency spectra and wavenumber spectra, converted by use of the mean aircraft ground speed (180 ms^{-1}).

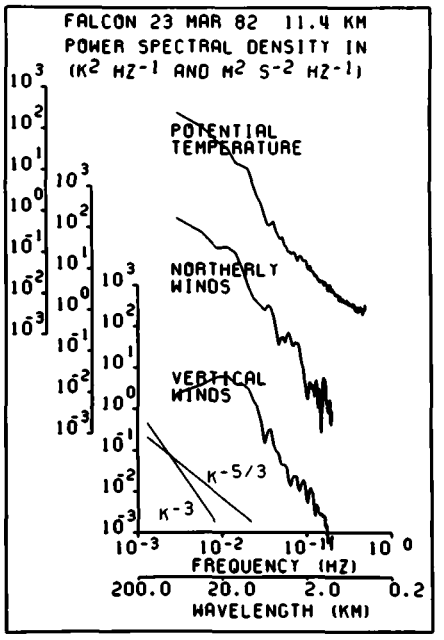

Fig. 14. As in Fig. 13 except for the 11.4 km level of the FALCON.

suggests a correlation of the form $w = -\mathrm{d}\theta/\mathrm{d}x$. Again, the coherence levels are close to 0.4 for the lower frequencies (not shown).

The v versus w correlations are important for the determination of the momentum fluxes. Simple wave theory and observations suggest that the momentum fluxes should be negative above mountains. This is the case for the phase of v versus w correlation spectra between 90° and 270° with a maximum at 180° with quadrature behaviour. For phases between −90° and +90°, we expect correlations greater than zero. In the present case, we found phases close to 180° at both levels. This indicates that the momentum fluxes during the present event were downwards. The coherence levels for this correlation spectrum are at 0.5 for both levels for the large scales.

The phase relationship which seems pretty clear in Figs. 11 and 12, shows up less clearly in the spectral diagrams (Figs. 15–17). This is due to the fact that the phase relationship is obvious for both levels at the lee side of the mountain and is shown up poorly at the windward side. Thus, the combination of both leads to a less clear issue than expected from considering just the behaviour at the leeward side.

6. The momentum flux

One of the most important quantitative measures of mountain wave intensity is the exchange of momentum between the atmosphere and the sloping lower boundary. This is equal to the wave drag which is the force exerted by the earth through differential pressures on the windward and leeward slopes. In this section, the eddy momentum flux integral $\int \rho\, v'w'$ is evaluated, where the primes represent deviations from the horizontal flight leg average. Again, the mean and the trend are removed by least-squares fitting. We calculate directly the relevant covariances by using

$$\int_{t=t_1}^{t=t_2} \rho\, v'w'C\, \mathrm{d}t.$$

The velocity C was chosen to be the true ground speed of the aircraft.

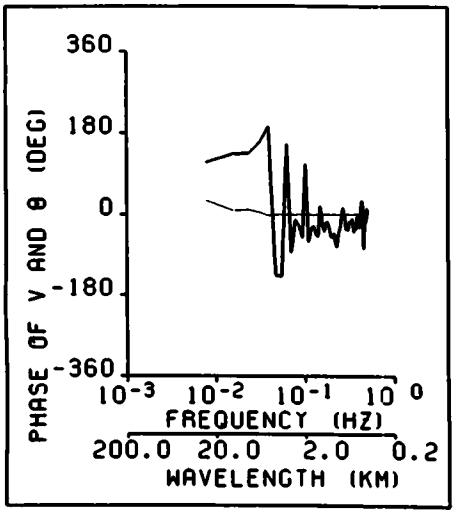

Fig. 15. Phase of the correlation spectrum of v and θ for the 4.0 km flight level of the P-3 (thin) and the 11.4 km flight leg of the FALCON (solid). A positive angle of less than 180° indicates that v leads θ in time. Phase angles are periodic over 360°.

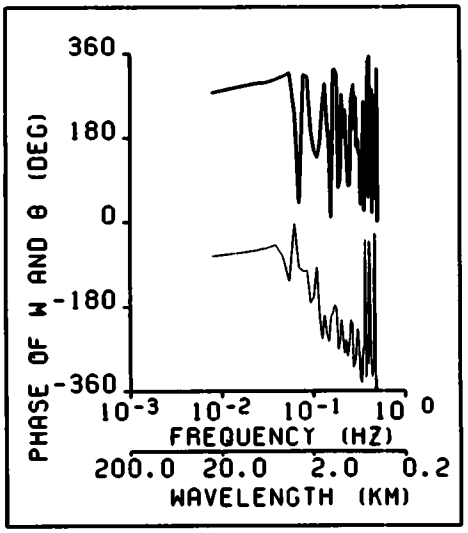

Fig. 16. As in Fig. 15 except for w and θ.

In Figs. 18–19, the running integrals of the momentum flux of all flight levels are portrayed. At all levels, the momentum flux is strongly negative (i.e. upgradient) as would be expected from mountain wave theory. In Fig. 20, we show the mean momentum flux for all levels. The plotted

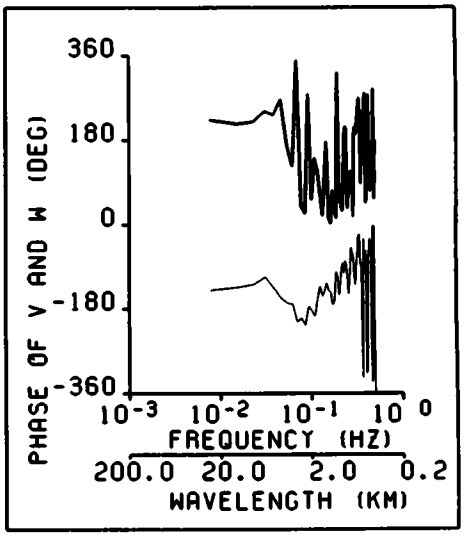

Fig. 17. As in Fig. 15 except for v and w.

values are those taken from the endpoints of the momentum flux curves shown in Figs. 18–19. Due to the general uncertainty and noise of momentum flux integrals, it is appropriate to average the lower four estimates and the upper four to obtain representative estimates for both layers. A strong increase of the flux was found at 6–10 km altitude with a decrease above and beneath this layer. The magnitude of the vertical flux of horizontal momentum is between 0.2 and 0.7 Pa. For the Colorado-case with waves of larger amplitude, values of 0.4 to 1.0 Pa were analysed, which agree well with our results for the flow over the Pyrenees.

The highest level flown by the FALCON was 12.0 km, corresponding to a height of approximately 14 km in the Colorado-case. During the latter event, a turbulent layer was observed close to 16 km. Thus, the highest leg of the FALCON was too low to touch the region where the momentum flux approaches zero. Thus, a turbulent layer with a strong wave-breakdown, where a removal of wave energy into turbulent energy occurs, is not found above the Pyrenees, but a strong decrease of momentum flux with height is analysed.

Eliassen and Palm (1960) have shown that an upward wave energy transfer is always combined with a downward momentum flux, and this flux is constant with height as long as there are no dissipative effects and there is steady-state behaviour. In our case there is a vertical divergence

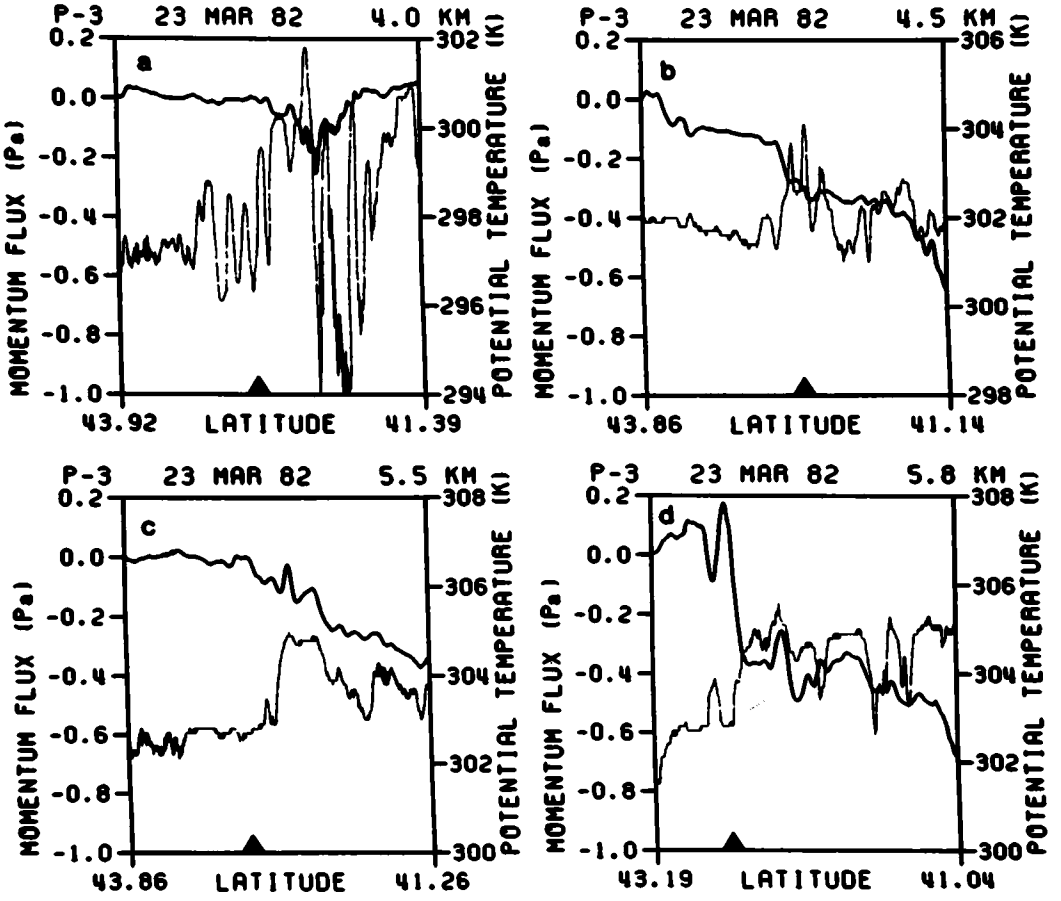

Fig. 18. Running spatial integral of momentum flux $\int \rho v'w'\,dx$ (fat) and potential temperature (thin) over the P-3 flight legs at 4.0 km (a), 4.5 km (b), 5.5 km (c) and 5.8 km (d). v' and w' are the deviations from the means and least squares trends. The spatial increment dx is taken to be equal to $C\,dt$, where C is the true ground speed of the aircraft. The mountain crest is indicated by the black triangle.

in the momentum fluxes. This is not an effect of the combination of two profiles measured 80 km apart, because both profiles have a similar shape. In the realistic airflow over the Pyrenees there are dissipative effects, so we should not expect strong constancy with height. Fig. 20 either shows the inapplicability of the steady-state assumption or demonstrates simply that the flight legs were not long enough to allow a clear separation of mean and fluctuating velocity, or both.

A further component of the drag force acting between the earth and the atmosphere is the frictional drag. The relative importance of this drag is illustrated by its magnitude of 0.2 Pa (for winter 45° N) assuming 300 km for the length of the forcing region (Kung, 1968). In our case, wave drag and frictional drag are almost equal in importance. The wave drag generated by the mountain corresponds close to the surface to the mountain drag. But, as pointed out by Smith (1978), there is no information about whether these two types of drag are correlated, perhaps inversely, leading to a partial compensation.

For the general circulation, the mountain torque is smaller than the frictional torque but not negligible. This computed mountain torque represents only the large-scale effects of mountain ranges with a resolution of at best 5° latitude. Thus, the evaluation remains of uncertain value because of its exclusion of scales smaller than hundreds of

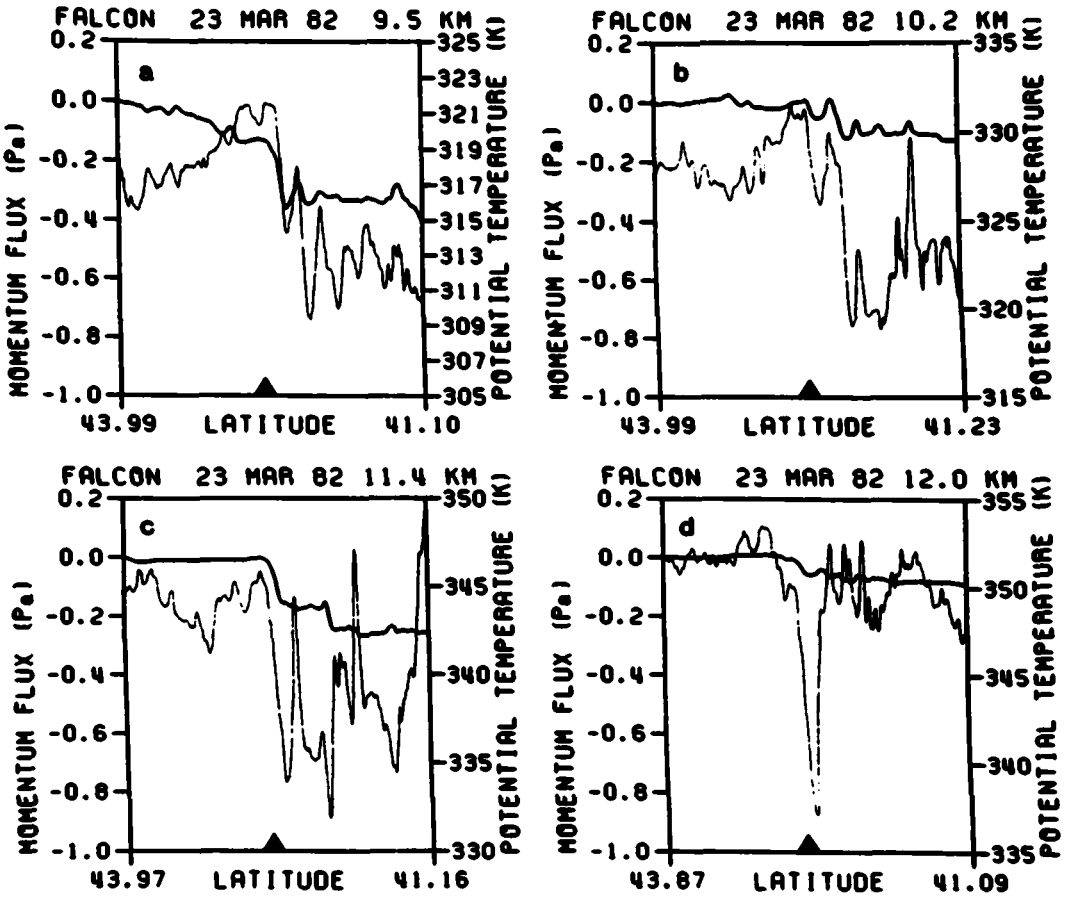

Fig. 19. As in Fig. 17 except for the FALCON flight legs at 9.5 km (a), 10.2 km (b), 11.4 km (c) and 12.0 km (d).

kilometers. Recently Oort and Bowman (1974) evaluated for 50° N a drag due to a large-scale motion of about 0.03 Pa for a scaling length of 300 km of the flight legs. The comparison of this magnitude with the magnitude of the mesoscale mountain drag shows the strong importance of the impact of mountains of the scale of the Pyrenees on the large scale flow in the free atmosphere.

As we have seen, close to the tropopause there is a vertical divergence in the momentum flux indicating dissipation. An estimation of dissipation rates comes from considerations of the large-scale energy budget. From the equations of motion, the removal of energy by dissipation can be expressed as

$$\varepsilon = \bar{u}\frac{\partial}{\partial z}\int \rho\, u'\, w'\, \mathrm{d}x.$$

with $\bar{u}$ the mean horizontal velocity of the corresponding layer. Assuming that a flux of 0.35 Pa, taken from Fig. 20, is removed at a depth of 40 mb, with a mean flow of 33 ms^{-1}, the computed energy removed is about 12W m^{-2}.

This magnitude of the momentum flux divergences suggests that the dissipation near the tropopause is by no means negligible. If distributed across Europe, a distance of about ten times our averaging length, the observed dissipation rate is 1.2W m^{-2}. Trout and Panofsky (1969) reported an average dissipation rate of 1.07W m^{-2} in the layer between 8 to 12 km. A comparison of this average dissipation rate with the estimate for the Pyrenees case shows that the measured values of dissipation above the Pyrenees have considerable significance for the larger scales of the atmosphere.

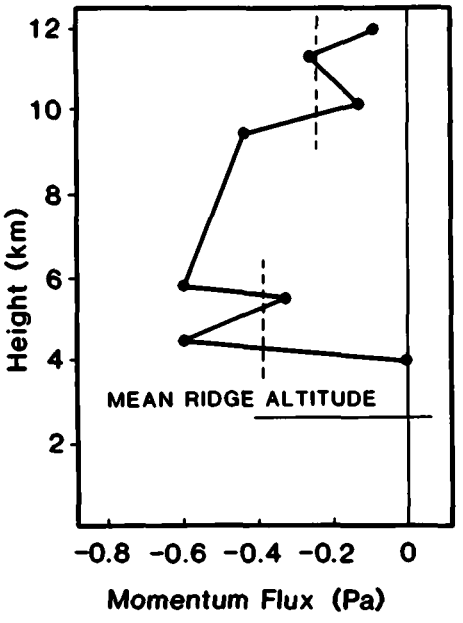

Fig. 20. Observed profiles of momentum flux obtained above in the Pyrenees on March 23, 1982. The abscissa is given in Pa and the height at the ordinate in km. The dashed lines represent averaged values of the lower four and upper four estimates.

7. Conclusion

The analysis of the data corroborates that the airflow over the Pyrenees on March 23, 1982 was an important mountain wave event. A rather strong wave in the flow is apparent in the lower and in the middle troposphere which becomes stronger with reversal phase in the vicinity of the tropopause. The character of the flow is fairly three-dimensional up to 7 km. Above this level the three-dimensional behaviour is less pronounced. As observed during foehn (Alps) and during chinook (Rocky Mountains), the impact of the barrier leads to a destabilization of the leeward atmosphere.

The observed momentum flux profile shows negative (downward) values at all levels, with a maximum of 0.7 Pa at 450 mb and a minimum of 0.1 Pa near the surface and near 200 mb. The observed features and the evaluated momentum flux values suggest that the Pyrenees case is similar to the event observed above the Rocky Mountains on February 17, 1970 analysed by Lilly and Kennedy (1973). However, the intensity of the waves is less strong than in the mountain wave event above the Rockies.

The observed wave drag was found to be of order 2 times the average frictional force per latitudinal meter exerted by the earth on the atmosphere. Energy budget estimations show substantial dissipation in the upper troposphere and the lower stratosphere. If the dissipation rate is distributed along 50° N across Europe, the observed dissipation is 1.2W m^{-2} which is of the same magnitude as the winter average value of 1.07W m^{-2} in the upper troposphere and the lower stratosphere. Thus, the event contributed substantially to the global momentum balance during its brief lifetime.

8. Acknowledgements

I would like to express my gratitude to the Airborne Mission Scientists of the ALPEX flights on March 23, 1982: W. Blumen (FALCON) and H. Pierrehumbert (P-3). H. Fimpel is thanked for the data processing of the FALCON-data. I am indebted to P. Kennedy, who provided me with the P-3 data. I wish to thank Joseph Egger, who read and commented on an earlier version of the paper, Doug Lilly and an anonymous reviewer whose criticisms were very helpful. Mrs. Jakob is thanked for the excellent job of preparing the drawings.

REFERENCES

Blumen, W. and Cox, K. W. 1984. Analysis of a stretched variable transformation of Scorer's equation for use of the mountain lee wave studies. *J. Atmos. Sci. 41*, in press.

Eliassen, A. and Palm, E. 1961. On the transfer of energy in stationary mountain waves. *Geofys. Publ. 22 No. 3*, 1–23.

Hoinka, K. P. 1980. Synoptic-scale atmospheric features and foehn. *Contrib. Atmos. Phys. 53*, 486–507.

Julian, P. J. 1975. Comments on the determination of significance levels of the coherence statistics. *J. Atmos. Sci. 32*, 836–837.

Kennedy, P. J. 1982. An ALPEX aircraft atlas. NCAR, Boulder, Co., July 1982.

Kuettner, J. P. ed. 1982. Preliminary Results of ALPEX. *GARP Publ. Ser.*, GARP-ALPEX Report No. 7.

Kuettner, J. P. and Lilly, D. K. 1968. Lee waves in the Colorado Rockies. *Weatherwise 27*, 180–198.

Kung, E. C. 1968. On the momentum exchange between the atmosphere and earth over the northern hemisphere. *Mon. Wea. Rev. 96*, 337–341.

Lilly, D. K. 1978. A severe downslope windstorm and aircraft turbulence event induced by a mountain wave. *J. Atmos. Sci. 35*, 59–77.

Lilly, D. K. and Kennedy, P. J. 1973. Observations of a stationary mountain wave and its associated momentum flux and energy dissipation. *J. Atmos. Sci.* **30**, 1135–1152.

Oort, A. H. and Bowman, H. D. 1974. A study of mountain torque and its interannual variations in the northern hemisphere. *J. Atmos. Sci. 31*, 1974–1982.

Smith, R. B. 1978. A measurement of mountain drag. *J. Atmos. Sci. 35*, 1644–1654.

Trout, D. and Panofsky, H. A. 1969. Energy dissipation near the tropopause. *Tellus 21*, 355–358.